Drawability of Circular Blank of Stainless Steel Sheets

Shigetoshi SHIMIZU*, Shunichi KAWANO*,
José MIAMOTO**, Mamoru MATSUO***

Abstract

This paper presents the experimental and theoretical study about the regions of wrinkling, fracture of sheet metal and limiting drawing ratio of the SUS-27 stainless steel sheet of 0.8 mm thickness fixing the tool dimensions, changing the diameter of blank and blank-holding pressure. Within the scope of the parameters adopted in this experiment, the experimental results agree fairly well with theoretical ones.

1. Introduction

Several theoretical and experimental analyses have been made by many authors[1)~9)] to define the drawability of the sheet metal about the relation between punch load and punch travel, wrinkling phenomena and breaking strength of sheet. With above study they become clear that the drawability of the sheet metal is affected by the following factors : (a) drawing form, (b) quality of sheet metal, (c) lubricant, (d) blank-holding pressure, (e) drawing speed and (f) thickness of sheet metal.

The principal objcet of this work is to study about the regions of wrinkling, fracture of sheet metal and limiting drawing ratio which is the ratio of the maximum blank diameter, that can be drawn successfully, to the punch diameter, using the deepdrawing of a circular blank by a flat-headed punch.

All the experimental work was made in the SUS-27 stainless steel sheet of 0.8 mm thickness fixing the tool dimensions, however changing the diameter of blank and blank holding pressure.

The theoretical relation between punch load and punch travel was followed the criterion proposed by Masuda and Murota[2)]. The theoretical breaking strength of sheet metal was followed the method proposed by Yamada[7)], and the analysis of the theoretical wrinkling phenomena was adopted Kikuchi's criterion[3)].

2. Experimental Work

Cylindrical cups were formed from circular blanks on a hydraulically operated "TF-102"

* Department of Technical Engineering
** Aço Inoxidável Fabril Guarulhos S. A. São Paulo, Brasil
*** Daikin Kogyo Co. Ltd.

sheet metal testing machine. The punch speed was hold about 0.10 mm/sec by hand. The principal dimensions of the sheet metal testing machine are shown in Table 1.

Table 1. Principal dimensions of testing machine.

maximum punch load	12 ton
maximum blank holding pressure	4 ton
punch diameter	40 mm
punch profile radius	8 mm
die diameter	45 mm
die profile radius	10 mm

The sheet material used in this work was SUS-27 (AIS 304) stainless steel which composition is shown in Table 2.

Table 2. Compositions of sheet material (%).

C	Si	Mn	P	S	Ni	Cr
0.07	0.48	1.11	0.026	0.009	8.92	18.56

The simple tension test was made in three dimensions, 0°, 90° and 45° taking the 0° for the roll direction, using the JIS-13 B testing pieces. The properties of the metal are shown in Table 3, and the true stress-strain diagrams are given in Fig. 1.

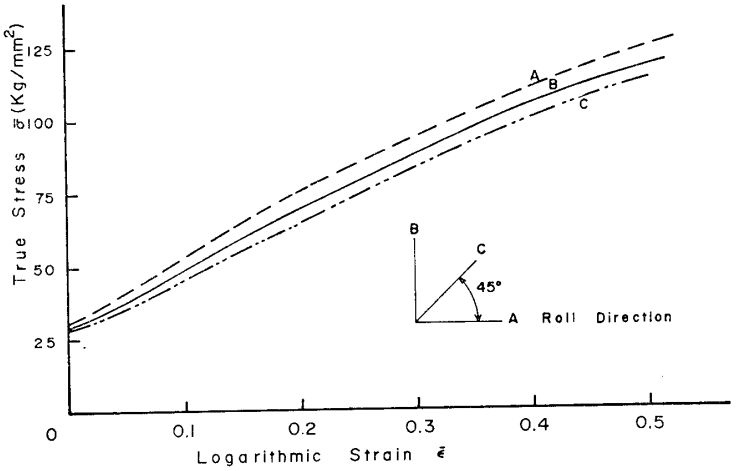

Fig. 1. True stress-strain diagrams of the material.

Table 3. Material properties.

Orientation to rolling direction	E kg/mm²	σe kg/mm²	F′ kg/mm²	F kg/mm²	n′	n
0°	1.4×10⁴	26.0	168.5	189.3	0.478	0.867
90°	1.4×10⁴	26.0	155.1	186.7	0.469	0.928
45°	1.4×10⁴	26.0	151.4	189.5	0.481	0.994

Note, F, n and F′, n′ are constants in the empirical equations $\sigma=F\bar{\varepsilon}^{n}$ and $\sigma=\sigma_e+F'\bar{\varepsilon}^{n'}$, respectively.

The blanks were lublicated on both side by using "Castrol-PS 158". The lublicant was diluted with water in the ratio of 1 : 1. The series of blank was 75.0, 81.0, 85.0 , 88.6 and 95.0 mm in the diameter. Each blank was tooled and polished, and their thickness was 0.8 mm.

Observing the wrinkling phenomena on the flange of blank, we used an apparatus as shown in Fig. 2, schematically. When the flange of blank starts wrinkling, the blank holder will be pussed down against the blank-holding pressure by the convex surface of flange, thus we can measure the displacement of the blankholder by using the optical lever. The observed minimum value of displacement was 0.001 mm by using this apparatus.

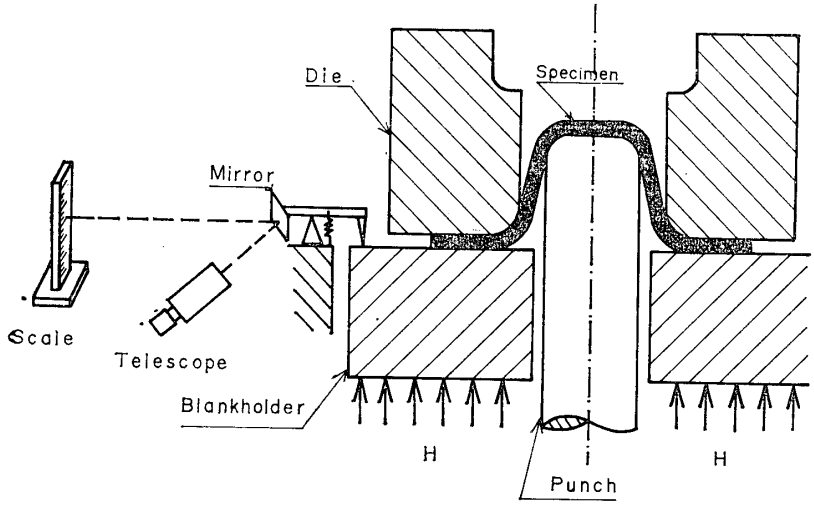

Fig. 2. Apparatus of measuring the wrinkling phenomena.

3. Numerical Calculations

Numerical analysis follows the method of solution proposed by Masuda and Murota[2] for an elastic-perfectly plastic solid and extended by authors for use with a work hardening material, as introduced in Appendix. The punch load P, punch travel Y and the blank radius of working blank r_0 are expressed by the following expressions using the parameter

ϕ which defines the adopted angle as shown in Fig. 3, assuming the coefficient of friction μ. (refer Appendix)

Notation

R_0 : initial radius of blank
r_0 : radius of working blank
r_1 : radius of die
r_2 : radius of punch
ρ_d : die profile radius
ρ_p : punch profile radius
ϕ_1 : adapted angle
σ_ϕ : stress component for the meridian direction in the die radius region
$a=r_1+\rho_d$
$b=r_2-\rho_p$

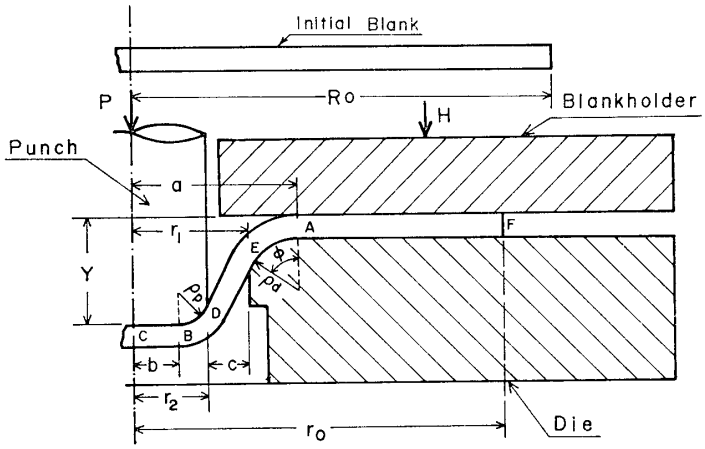

Fig. 3. Geometry of cup drawing.

$$P=2\pi r_1 t(\sigma_\phi)_{\phi=\phi_1} \sin\phi_1 \tag{1}$$

$$Y=(\rho_p+\rho_d)(1-\cos\phi_1)+(r_1-r_2)\tan\phi_1 \tag{2}$$

$$r_0=[R_0{}^2-(a^2-b^2)(\sec\phi_1-1)+2(a\rho_d+b\rho_p)(\tan\phi_1-\phi_1)+(\rho_p{}^2-\rho_d{}^2)(\sec\phi_1+\cos\phi_1-2)]^{1/2} \tag{3}$$

The theoretical breaking strength of sheet metal is followed the method proposed by Yamada[7], as

$$P_{max}=A_0\ \sigma_T\left(\frac{2}{\sqrt{3}}\right)^{n+1} \tag{4}$$

where σ_T is the tensile strength of material, and A_0 is the sectional area of blank at the junction of punch profile with punch stem.

And the minimum blank-holding pressure H_{min} for wrinkling of flange is adopted Kikuchi's criterion[3] expressed as follows

$$H_{min}=0.55\pi\ \frac{r_0 t^2}{\rho_d}\ \sqrt{B\sigma_t} \tag{5}$$

where $\sigma_t=\left(A+B\frac{u_0}{r_0}\right)\frac{a}{r_0-u_0}$

$\sigma=A+B\varepsilon$

A, B : coefficient of plasticity of material

In this study, the numerical calculation of the deep drawing of sheet metal including the wrinkling and fracture mechanism by the electronic computer "FACOM 230—60", which flow chart is shown in Fig. 4.

We adopted the values of material properties of 45° direction for the roll in Table 3 to the following calculations.

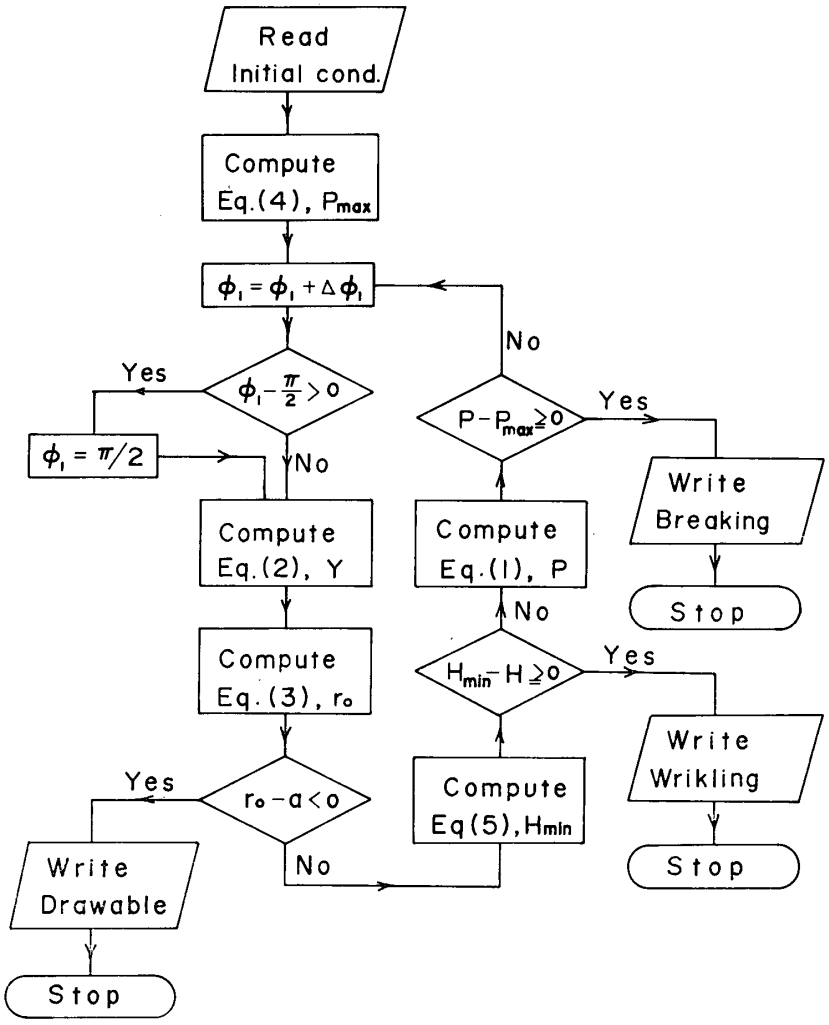

Fig. 4. Flow chart of numerical calculation of deep drawing by electronic computer.

4. Experimental and Theoretical Results

The deep drawing tests were performed by changing the blank-holding pressure and diameter

Table 4. Combination of blank-holding pressure H and diameter of blank R_0.

R_0(mm) / H(ton)	75	81	85	88.6	95	R_0(mm) / H(ton)	75	81	85	88.0	95
0.10	○				○	0.80					○
0.20		○	○	○	○	0.85					○
0.25					○	1.00	○	○	○	○	○
0.30			○		○	1.50					○
0.40		○	○	○	○	2.00	○	○	○	○	○
0.50	○				○	2.50					○
0.60					○	3.00	○	○	○	○	○
0.70					○	3.50					○
0.75					○	4.00	○	○	○	○	○

of blank as shown Table 4. The typical diagrams of punch load versus punch travel are given in Fig. 5. The punch speed was controled manually, and its mean speed was about 0.10 mm/sec. Changing the blankholding pressure from 0.1 ton to 4 ton, we tested for blank diameter of 95.0 mm, for all the cases, the fracture occured near the junction of the punch profile with the punch stem as shown Photograph 1 (a) and the experimental maximum punch load was about 8.4 ton, on the other hand the theoretical fracture punch load was 8.8 ton by Eq. (4).

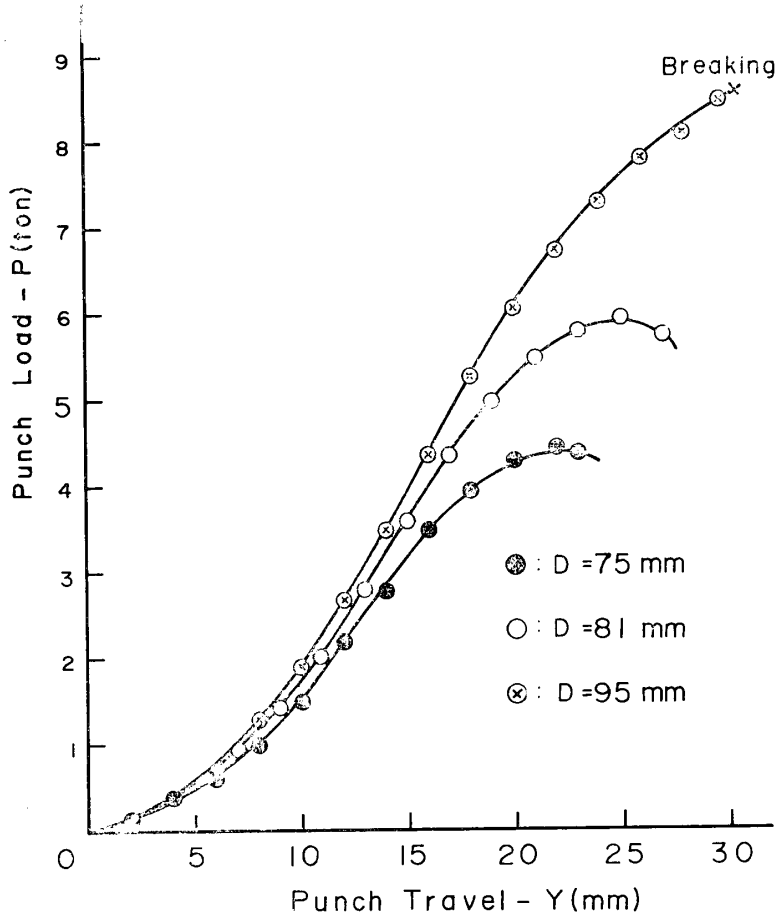

Fig. 5. Experimental diagrams of punch load P versus punch travel Y.

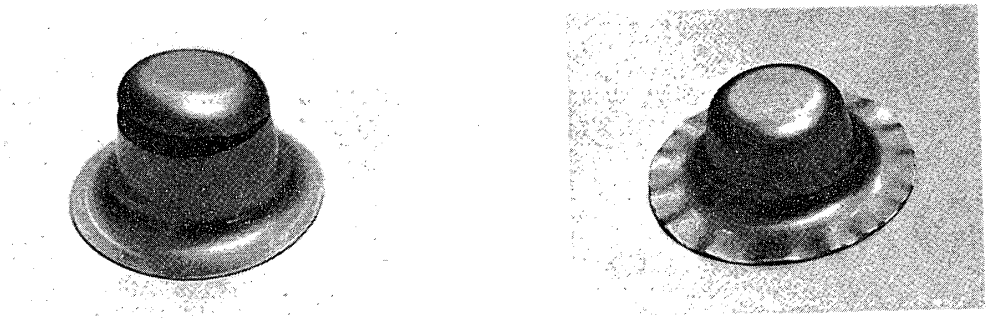

(a) Mode of fracture cup drawing.

(b) Mode of wrinkling cup drawing.

Photograph 1

In Fig. 8, we show also the theoretical working limit of punch load by using Eq. (4).

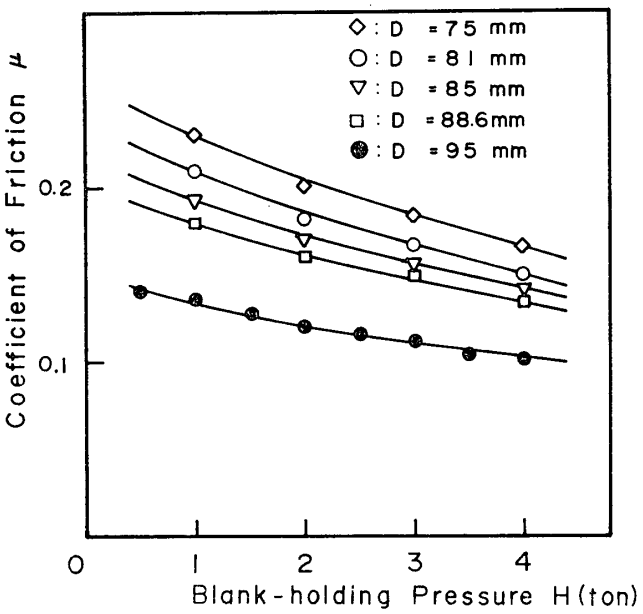

Fig.7. Apparent coefficient of friction μ.

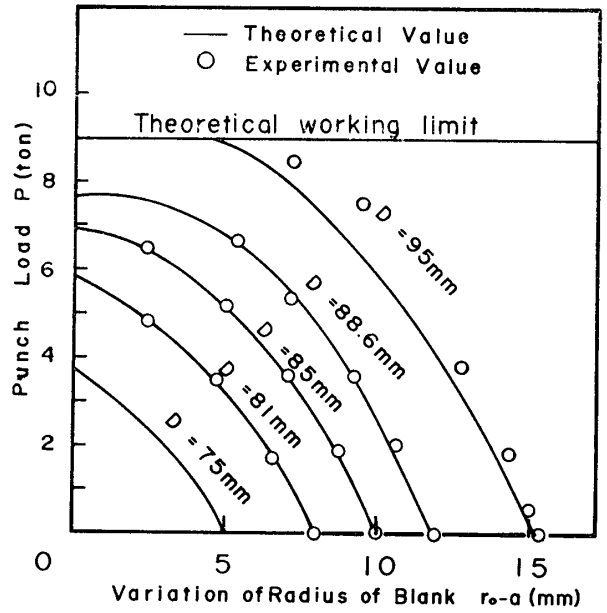

Fig.8. Variation of radius r_0-a of blank during the operation of deep drawing.

In Fig. 9, we show the diagrams of punch load P versus blank-holding pressure H for all the refered blank diameter, which are obtained from experimentally and theoretically simultaneously. We can determine the regions of working limiting and the wrinkling of flange from Fig. 9. The theoretical working limiting values result greater than the experimental ones, on the contrary the theoretical wrinkling limiting values are slightly less than the experimental results.

For the blank diameter of 90.0 mm, we could not find the fracture at the blankholding pressure slightly less than 2.0 ton, but the wrinkling of flange occured as shown Photograph 1 (b). The same tests were made also for the blank diameters of 88.6, 85.0, 81.0 and 75.0 mm, which never fractured for any cases.

As the value of coefficient of friction μ was unknown in this calculation, we assumed the several values for μ, and calculated the value of punch load P and punch travel Y by using Eqs. (1) and (2), respectively. As an examaple, the calculation results of P and Y to 2.0 ton blankholding pressure and the blank diameter of 95.0mm, as shown in Fig. 6, we can make accord the theoretical diagram with the experimental one, if we take the suitable value to μ, say $\mu=0.1$.

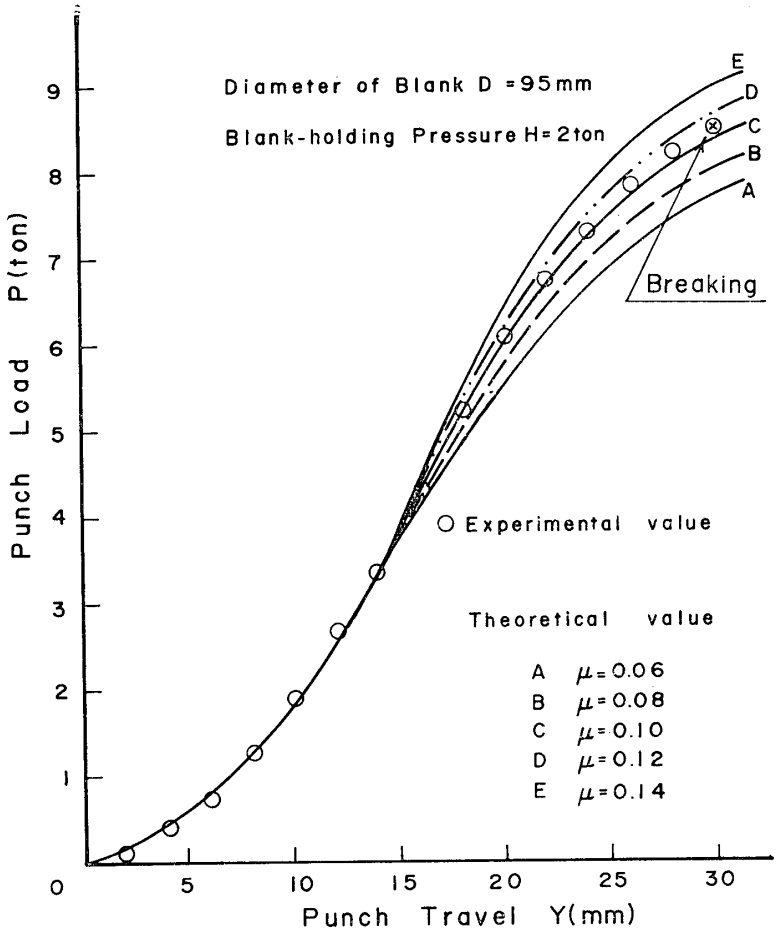

Fig.6. Theoretical diagrams of punch load P versus punch travel Y with varying coefficient of friction μ.

These apparent coefficients of friction are affected by the blankholding pressure and blank diameter as shown Fig. 7. Increasing the blankholding pressure, the value of coefficient of friction decreases, but the variations not so large. The other hand, the smaller the blank diameter is, the more the value of coefficient increases, and it takes the value between $\mu=0.08\sim0.24$.

Using Eq. (3), the variation of radius r_0-a of blank during the operation of deep drawing are calculated for the various blank diameter using the apparent coefficient of friction obtained from Fig. 7, and make a comparison with the experimental results as Fig. 8.

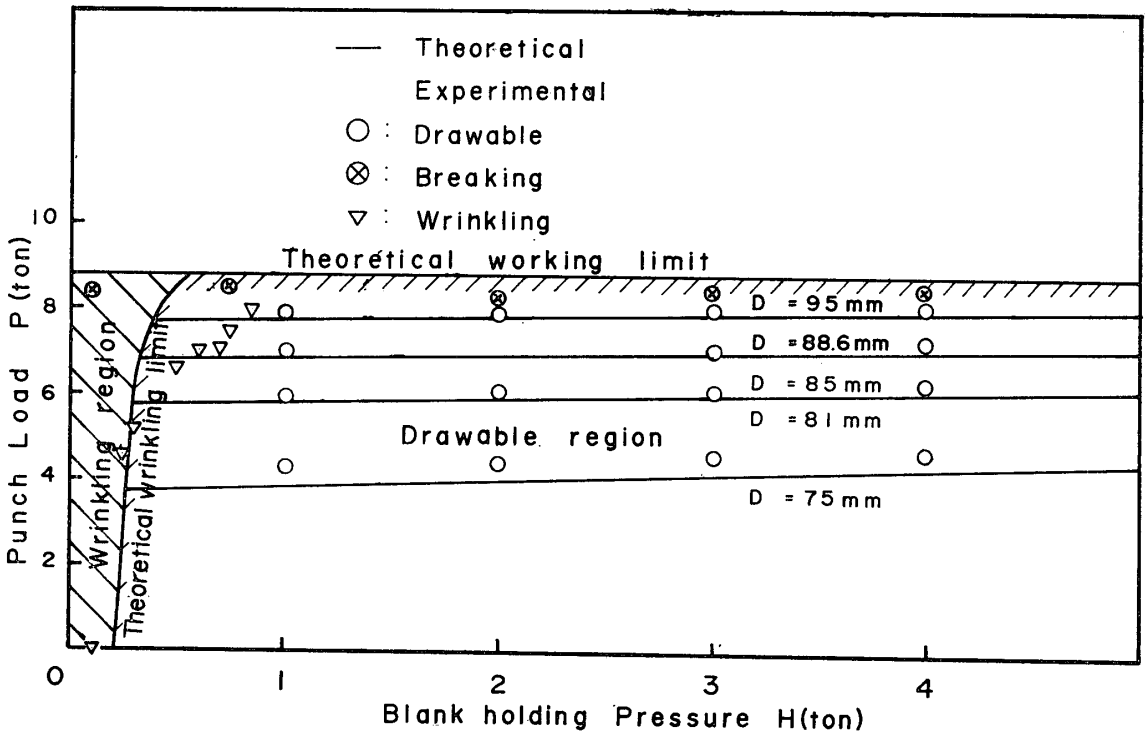

Fig.9. Diagrams of punch load P versus blank holding pressure H varying blank diameter.

Reference

1) R. Hill : "The Mathematical Theory of Plasticity", Clarendon Press, Oxford, (1950)
2) M. Masuda and T. Murota : Trans. J. S. M. E., 18—68, (1952), pp. 133—139
3) Y. Kikuchi : Jour. J. S. M. E., 56—409, (1953), pp. 110—116
4) M. Miyagawa : Trans. J. S. M. E., 23—130, (1957), pp. 390—407
5) Y. Kasuga and N. Nozaki : Trans. J. S. M. E., 24—146, (1958), pp. 720—732
6) N. Kawai : Jour. J. S M. E., 26—166, (1960), pp. 850—873
7) Y. Yamada : Jour. J. S. M. E., 67—542, (1964), pp. 453—465
8) Japan Sheet Metal Forming Research Group : Jour. J. S. T. P., 13—132, (1972), pp. 53—59
9) M. G. El-Sebaie and P. B. Mellor : Int. J. Mech. Sci., 14—9, (1972), pp. 1302—1313
10) E. Siebel : "Die Formgebung im bildsamen Zustande", (1932)

Appendix : Basic Equations in Deep Drawing

The following equations are for pure radial drawing of a circular blank of isotropic material. The configurations of deep drawing and an element IJKM cut out from the die radius region are shown in Fig. A-1, where σ_ϕ and σ_θ are stress components which act normally to the sides JI (KM) and KJ (MI), respectively, while t and r are the current thickness and radius of an element, and q is normal pressure on the element IJKM.

In the die radius region FA, the equation of equilibrium is

$$\frac{d(rt\sigma_\phi)}{d\phi}-\mu rt\sigma_\phi+(\cos\phi+\mu\sin\phi)\rho_d t\sigma_\theta=0 \qquad \text{(A-1)}$$

where μ is the coefficient of friction, and ρ_d is the die profile radius.

While the following equation of equilibrium is obtained in the flange region, where σ_r

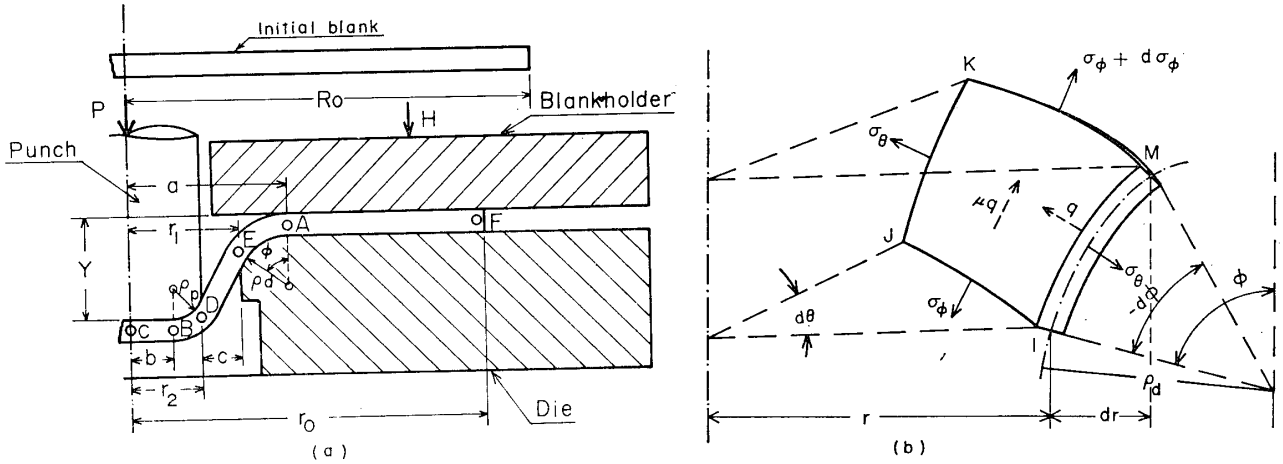

Fig. A-1. Geometry and equilibrium conditions in cup drawing.

is the current outward radial stress component.

$$\frac{d(rt\,\sigma_r)}{dr} - t\,\sigma_\theta = 0 \qquad \text{(A-2)}$$

Taking the current outward radial displacement in the flange region FA u and corresponding outward and tangential strain as ε_r and ε_θ, then

$$\left.\begin{aligned} \varepsilon_r &= \frac{du}{dr} \\ \varepsilon_\theta &= \frac{u}{r} \end{aligned}\right\} \qquad \text{(A-3)}$$

Since the die profile radius ρ_d is small compared with the radius of die r_1, strain of meridian direction in the die radius region ε_ϕ is

$$\varepsilon_\phi = \frac{du}{dr} \qquad \text{(A-3')}$$

Neglecting the variations of blank thickness and its volume, we obtain the following equation from Eq. (A-3),

$$\varepsilon_r + \varepsilon_\theta = \varepsilon_\phi + \varepsilon_\theta = \frac{du}{dr} + \frac{u}{r} = 0 \qquad \text{(A-4)}$$

According to the total strain theory, the relation between stress and strain is expressed by the following equation.

$$\varepsilon = \left(\frac{\sigma - \sigma_e}{F}\right)^{1/n} \qquad \text{(A-5)}$$

Where, F, n and yielding stress σ_e are constants which are determined from the work-hardening characteristics of material shown in Table 3.

Thus the current outward radial strains ε_r and ε_ϕ may be written as

$$\left.\begin{aligned} \varepsilon_r &= \left(\frac{\sigma_r - \sigma_\theta - \sigma_e}{F}\right)^{1/n} \\ \varepsilon_\phi &= \left(\frac{\sigma_\phi - \sigma_\theta - \sigma_e}{F}\right)^{1/n} \end{aligned}\right\} \qquad \text{(A-6)}$$

If it is assumed reasonably that all of the blank-holding pressure H is exerted at the

rim of blank during deep drawing, the boundary conditions a re

$$\left.\begin{aligned}(u)_{r=r_0} &= -u_0\\ (\sigma_r)_{r=r_0} &= \frac{\mu H}{\pi r_0 t}\end{aligned}\right\} \qquad \text{(A-7)}$$

where u_0 is the absolute value of radius displacement u at $r=r_0$, and r_0 is the radius of working blank.

From Eqs. (A-2), (A-3), (A-4), (A-6) and (A-7), following expressions for the stress components in the die radius region EA in Fig. A-1 are obtained.

$$\left.\begin{aligned}\sigma_r &= \sigma_e \ln\frac{r_0}{r}+\frac{(u_0 r_0)^n}{2n}F\left(\frac{1}{r^{2n}}-\frac{1}{r_0^{2n}}\right)+\frac{\mu H}{\pi r_0 t}\\ \sigma_\theta &= \sigma_e\left(\ln\frac{r_0}{r}-1\right)+\frac{(u_0 r_0)^n}{2n}F\left(\frac{1-2nr^n}{r^{2n}}-\frac{1}{r_0^{2n}}\right)+\frac{\mu H}{\pi r_0 t}\end{aligned}\right\} \qquad \text{(A-8)}$$

On the other hand, the stress component σ_ϕ in the radius region is

$$\sigma_\phi = e^{\mu\Phi(\phi)}\left[e^{-\mu\Phi(0)}\sigma_{ra}+\left\{\sigma_e+\left(\frac{u_0 r_0}{r^2}\right)^n F\right\}\int_0^\phi \frac{\rho_d(\cos\phi+\mu\sin\phi)}{a-\rho_d\sin\phi}e^{-\mu\Phi(\phi)}d\phi\right] \qquad \text{(A-9)}$$

where

$$\Phi(\phi)=\int\left(1-\frac{\rho_d\sin\phi}{a-\rho_d\sin\phi}\right)d\phi$$

$$=2\left\{\phi-\sqrt{1+m^2}\tan^{-1}\left(\sqrt{1+m^2}\tan\frac{\phi}{2}-m\right)\right\}$$

$$m=\rho_d/\sqrt{a^2+\rho_d{}^2}$$

$$a=r_1+\rho_d$$

$$\sigma_{ra}=\sigma_e\ln\frac{r_0}{a}+\frac{(u_0 r_0)^n}{2n}F\left(\frac{1}{a^{2n}}-\frac{1}{r_0^{2n}}\right)+\frac{\mu H}{\pi r_0 t}$$

Considering the influence of bending at the die shoulder, the Eq. (A-9) is modified by using E. Siebel's method[10], as follows

$$\sigma_\phi = e^{\mu\Phi(\phi)}\left[e^{-\mu\Phi(0)}\sigma_{ra}+\left\{\sigma_e+\left(\frac{u_0 r_0}{r^2}\right)^n F\right\}\int_0^\phi \frac{\rho_d(\cos\phi+\mu\sin\phi)}{a-\rho_d\sin\phi}e^{-\mu\Phi(\phi)}d\phi\right]$$
$$+(1+e^{-\mu\phi_1})\frac{t}{4\rho_d}\sigma_e \qquad \text{(A-10)}$$

where ϕ_1 is the adapted angle in the die profile. Therefore, the punch load P is expressed as

$$P=2\pi r_1 t(\sigma_\phi)_{\phi=\phi_1}\sin\phi_1 \qquad \text{(A-11)}$$

If the side wall region DE is conicalface, from the geometric condition, the punch travel Y is

$$Y=(\rho_p+\rho_d)(1-\cos\phi_1)+(r_1-r_2)\tan\phi_1 \qquad \text{(A-12)}$$

where ρ_p is the punch profile radius, and r_2 is the radius of punch.

Using the conditions of the thickness and its volume are constant, the radius of working blank is

$$r_0=\left[R_0{}^2-(a^2-b^2)(\sec\phi_1-1)+2(a\rho_d+b\rho_p)(\tan\phi_1-\phi_1)\right.$$
$$\left.+(\rho_p{}^2-\rho_d{}^2)(\sec\phi_1+\cos\phi_1-2)\right]^{1/2} \qquad \text{(A-13)}$$

where $b=r_2-\rho_p$.

(昭和48年4月18日受理)